TESTING AN ENERGY BALANCE MODEL FOR ESTIMATING ACTUAL EVAPOTRANSPIRATION USING REMOTELY SENSED DATA

R. J. Gurney
Department of Civil Engineering
University of Maryland
College Park, MD 20740

P. J. Camillo
SAR
6811 Kenilworth Avenue
Riverdale, MD 20737

ABSTRACT

An energy-balance model is used to estimate daily evapotranspiration for 3 days for a barley field and a wheat field near Hannover, Federal Republic of Germany. The model was calibrated using once-daily estimates of surface temperatures, which may be remotely sensed. The evaporation estimates were within the 95% error bounds of independent eddy correlation estimates for the daytime periods for all 3 days for both sites, but the energy-balance estimates are generally higher; it is unclear which estimate is biassed. Soil moisture in the top 2 cm of soil, which may be remotely sensed, may be used to improve these evaporation estimates under partial ground cover. Sensitivity studies indicate the amount of ground data required is not excessive.

INTRODUCTION

Evaporation and soil-moisture status are important hydrological parameters which are difficult to estimate conventionally over large areas. There are some indications that remotely-sensed measurements may be able to assist in their estimation for these large areas (e.g., Rosema et al., 1978; Schmugge et al., 1980; Soer, 1980). One remotely-sensed measurement, of the surface temperature, may be used in numerical energy-balance models of the atmospheric boundary layer and upper soil to make inferences of several hydrological parameters of interest, including soil-moisture status and evapotranspiration. The principle of these models is to solve the equation:

$$S = R_N + L \cdot E + H \qquad (1)$$

where R_N is the net radiation; $L \cdot E$ and H the latent and sensible heat flux across the atmospheric boundary layer, respectively; and S is the soil heat flux. L is the latent heat of vaporization and E is the evapotranspiration flux. Each of these terms depends partly on the surface temperature, and on a set of boundary conditions such as the air temperature, the vapour pressure and the wind speed at some level above the surface, the incoming radiation and the temperature at some level in the soil. Given measurements of the boundary conditions, the surface temperature may be estimated, compared with remotely-sensed measurements of the surface temperature, and the two made to agree by parameter fitting. As remotely-sensed measurements are likely to be available only a few times daily in an operational scheme because of orbital constraints, and yet daily means or totals are of most use, the parameters are usually fitted at the times when remotely-sensed data are available and used for all simulation times during a day.

An extension of this type of model was described by Camillo et al. (1983), where both the energy and moisture balances were modelled for a bare soil surface. The equations are solved using a predictor--corrector optimization scheme. This model has advantages over previous models of greater computational efficiency and stability and of greater physical realism for bare soil. In a test using data from an experiment in the Federal Republic of Germany, the agreement between estimated and measured temperatures was better than 1 K and was most sensitive to two parameters, the surface roughness and the thermal conductivity of the soil solids. However, most of the earth's land surface is vegetated, and so extensions to the original model must be made in order to handle vegetated surfaces satisfactorily.

There are several problems with dealing with vegetated surfaces, including energy exchanges within a vegetated canopy and partitioning the energy and moisture exchanges between the plants and the soil surface. The classical way to estimate transfer across the boundary is to find relationships between measurable variables which may be explained by introducing combinations of resistances to movement, analogous to Ohm's law (Shuttleworth, 1976). For vegetation canopies this approach easily introduces large numbers of additional parameters. For a practical application using remotely-sensed data, it is better to have a few parameters which may be updated regularly (daily or even more frequently with spacecraft-borne sensors) rather than to try to

estimate many parameter values from a close succession of intensive ground measurements and then use them for long periods of time. A method such as described here may give reliable evapotranspiration estimates and error bars over large areas with minimal ground data.

The additions to the bare soil model required to model vegetated surfaces and a discussion of the simplifications required from the complex resistance models is described next.

MODEL DESCRIPTION

As in Camillo et al. (1983), the net radiation was measured, and the other components of the surface energy balance were modelled, as follows:

$$L \cdot E = - C_1 U_a (e_s - e_a) \tag{2}$$

$$H = - \gamma \, C_1 U_a (T_s - T_a) \tag{3}$$

$$S = - \lambda_1 (T_1 - T_s)/Z_1 \tag{4}$$

where T_s is the surface temperature; T_a the air temperature; e_s the surface vapour pressure; e_a the atmospheric vapour pressure; U_a the wind speed; and γ the psychrometric constant. λ_1, T_1 and Z_1 are the thermal conductivity, temperature at the center and depth to the center of the first layer, respectively.

The constant C_1 in Eqs. (2) and (3) is the bulk diffusion coefficient for neutrally stable atmospheric conditions which was used in the bare-soil simulations. A more complete evapotranspiration model which includes a plant resistance would be formulated as follows:

$$L \cdot E = - (\rho C_p/\gamma)[e_s - e_a)/(r_a + r_s)] \tag{5}$$

where ρ and C_p are the density and heat capacity of air; respectively, and r_a and r_s are aerodynamic and stomatal resistances, respectively. Under neutrally stable conditions, the aerodynamic resistance may be modelled (Brutsaert, 1982) as:

$$r_a = \frac{\ln^2(z/z_o)}{k^2 U_a} \tag{6}$$

where z is the height at which the meteorological data are measured; z_o is the roughness length; and k is von Karman's constant. Putting this resistance into Eq. (5), rearranging, and comparing to Eq. (2) gives:

$$C_1 = \frac{\rho C_p k^2}{\gamma \ln^2(z/z_o)(1 + r_s/r_a)} \tag{7}$$

The easiest application of this type of model using remotely-sensed data requires the bulk diffusion parameter C_1 to be constant between calibration times. This paper provides the presentation of the model, assuming a constant C_1 but allowing evaporation to be less than potential through constraints on the water balance through the soil-moisture flux. The model is tested by comparing the estimates of evaporation produced by the model against those produced by a more conventional eddy correlation and energy-balance approach for one set of ground conditions in the F.R.G. Further testing of the model under different conditions is clearly desirable.

For C_1 to be considered a constant, Eq. (7) shows either that the stomatal resistance must always be small when compared to the aerodynamic resistance, or that the ratio of the two must always be constant. Neither of these conditions is likely to be met, especially for stressed vegetation. However, there are mathematically- and physically-based reasons for taking this position, in addition to the simplicitly required for remote-sensing applications: (1) there must be some constant value of C_1 which, when used in Eqs. (2) and (3), will give the correct value for evapotranspiration integrated over some time period; and (2) an increase in stomatal resistance is accompanied by an increase in the surface temperature, due to the reduction in the latent heat flux. Thus, we can bypass fitting on the stomatal resistance, since the feedback mechanisms (the heat balance at the soil surface, Eqs. (1-4)) couple its behavior to that of the surface temperature, to which we are fitting. Eq. (7) shows that increasing, r_s should cause a smaller C_1, precisely the behaviour found in this study.

The soil heat flux term (Eq. (4)) may be rewritten to solve for T_s:

$$T_s = (z_1/\lambda_1)S + T_1 \tag{8}$$

Substituting the heat-balance equation (Eq. (1)) into this equation gives:

$$T_s = T_1 + (z_1/\lambda_1)[R_N(T_s) + L \cdot E(T_s) + H(T_s)] \tag{9}$$

Solving for T_s also gives the heat and moisture upper-boundary fluxes of the soil, S and E, respectively. These are used with the soil-moisture (q_θ) and heat (q_h) fluxes in the soil profile, computed from soil physical properties and temperature and moisture profiles, to solve the equations for temperature and moisture within the soil:

$$dT/dt = - C^{-1}(\partial q_h/\partial z) \tag{10a}$$

$$d\theta/dt = - \partial q/\partial z_\theta \tag{10b}$$

where θ is the volumetric moisture content; and C the volumetric heat capacity of the soil. The general layout of the soil model is described by Camillo et al. (1983).

In Eq. (2), E is the total evapotranspiration demand (cm s^{-1}), which for vegetated surfaces must be divided into an evaporation flux E_s from the soil surface and a transpiration flux E_p from the plants. The iterative structure of this model is used to facilitate this. A constant fraction of this demand function E is allocated to the soil evaporation E_s. If the soil-moisture supply cannot support this potential, E_s is reduced to the flux supplied to the first layer from below (Hillel, 1980). Then the transpiration, E_p, is set equal to the difference between E and E_s. If the plant is stressed so that this demand cannot be met, E_p is set to zero. Finally, E is reset to the sum of E_s and E_p. Thus, non-potential evapotranspiration is modelled by allowing the demand to match the supply, as defined by the soil-moisture extraction terms of the model, rather than as is conventionally done by reducing the atmospheric demand function directly, using a resistance formulation and then assuming that this demand can be met.

The model of the transpiration E_p is provided by an estimate of the crown potential, estimated using a root-water extraction model described in detail by Camillo and Schmugge (1983), and comparing this estimate of the crown potential to the atmospheric demand. The root model provides an additional term W in the soil-moisture flux Eq. (10b), so that:

$$d\theta/dt = - \partial q/\partial z_\theta - W \tag{11}$$

The model for the sink term W is:

$$W(z,t) = [\phi_s(z) - \phi_p(t)]/[\Omega_s(z) + \Omega_p(z)] \tag{12}$$

where $\phi_s(\theta,z)$ is the total potential energy of the soil water (the sum of the gravitational and matrix potential); $\phi_p(t)$ is the plant potential, or crown potential, which is allowed to vary with time but which is assumed constant with depth; Ω_s is the soil resistance; and Ω_p is the plant resistance. The soil resistance Ω_s may be modelled as:

$$\Omega_s = 1/[K(\theta)R(z)] \tag{13}$$

where $K(\theta)$ is the hydraulic conductivity (cm s^{-1}); and R(z) is the relative root density (cm^{-2}), and the resistance to flow in the roots may be modelled as:

$$\Omega_p(z) = r/R(z) \tag{14}$$

where r is the specific resistance, the inverse of the hydraulic conductivity in the roots (Hillel, 1980). Rearranging and substituting in Eq. (12) gives the sink term for each layer:

$$W_i = [K_i R_i(\psi_i - z_i - \phi_p)]/(1 + rK_i) \tag{15}$$

where ψ_i is the matrix potential; and $- z_i$ is the gravitational potential of moisture in the ith layer. R_i is often considered as the length of active roots per volume of soil, although there is no conclusive experimental evidence

about this. However, the relative root density appears more important than the absolute values at any depth, because the model only requires that R(z) represent the relative ability of the roots to absorb water at each depth.

The crown potential ϕ_p is modelled as a response to the atmospheric evapotranspiration demand function, and is computed by requiring that the integral of the sink terms over the soil profile be equal to this demand function E_p. Thus, for a profile divided into N layers, of thickness dz_j:

$$E_p = -\sum_{j=1}^{N} W_j dz_j \tag{16}$$

Inserting W_j from Eq. (15) into Eq. (16) and solving for the crown potential gives:

$$\phi p(t) = \frac{E_p(t) + \sum_{j=1}^{N} [K_j R_j (\psi_j - z_j) dz_j / (1 + rK_j)]}{\sum_{j=1}^{N} [K_j R_j dz_j / (1 + rK_j)]} \tag{17}$$

Once the crown potential is evaluated, the sink term may be evaluated for each layer using Eq. (15). To allow for the evidence that water flux from plants to the soil is negligible (Molz and Peterson, 1976), any negative sink terms W_j are set to zero and the remaining positive terms are reduced by the scale factor to satisfy Eq. (16).

Even though the transpiration model does not include stomatal resistance, a rudimentary mechanism does exist to model extreme plant stress. For periods of large demand or dry-soil conditions, the magnitudes of E_p and ψ_j (or possibly both) in Eq. (17) will be large, giving a large magnitude for the crown potential. There is a limit below which this negative potential cannot go, and if ϕ_p from Eq. (17) exceeds this limit, it is reset to equal the limit. As the soil dries further ϕ_s will become more negative, with no compensating change in ϕ_p possible; eventually the sink terms (Eq. (15)) will become negative and are, therefore, set to zero. In this way, the large stress modelled by a lower limit for ϕ_p may eventually cause transpiration to cease.

MODEL VALIDATION

The model has a somewhat different structure and philosophy from existing models of evapotranspiration, and so extensive validation of the approach is required for many different vegetation types under many different conditions. The validation described here is somewhat limited, being for wheat and barley crops under near-potential conditions for a site in the F.R.G., the data being taken in June 1979. The model must work well under these conditions if it is to have any general application. Although the surface temperature

data were collected for small areas only in this intensive measurement campaign, the data were exactly analagous to the soil surface temperatures that may be collected over large areas by remotely-sensed methods.

The data used to validate the model were taken during the experiment performed in Ruthe, F.R.G., in the summer of 1979. The Joint Measuring Campaign 1979 in Ruthe was organized to study the water budget of an agricultural area, and to explore the potential of remote sensing in regional water-balance studies (van der Ploeg et al., 1980). The experiment was undertaken as part of the Tellus Project, under the auspices of the Joint Research Centre, Ispra, Italy, of the European Economic Community. The Tellus Project was also one of the investigations of the NASA Heat Capacity Mapping Mission. An area of ~ 4 x 4 km, 15 km south of Hannover, F.R.G., was used for this experiment. The area, near Ruthe, has little relief in an open landscape with few trees, bushes, buildings or other windbreaks. The soils, developed in a Pleistocene loess ~ 2 m thick, are very homogeneous over large areas. The individual fields are large, with an average size of ~ 7.5 ha.

The data used in this study came from wheat and barley fields. Soil surface temperatures and soil temperature profiles were collected, together with gravimetric soil-moisture data and information about soil thermal conductivity and heat capacity, and net radiation, and wind speed, air temperature and vapour pressure profiles. These data were collected largely by the Institute of Hydrology and the University of Reading, Great Britain.

The root mean square error between measured and estimated surface temperatures for each day for both wheat and barley are given in Table 1 for a variety of bulk diffusion coefficients C_1 and an evaporation fraction f_s of zero. Taking the wheat field as an example for which data for two measurement sites, D and G, are available, it may be seen that there is a minimum root mean square error against site D temperature measurements for a value of C_1 of ~ 10^{-5} on each day, while for site G the root mean square error function is rather flat because the measured temperatures are usually below the estimated values, while the meteorological measurements used are more representative of those at site D. Similar conclusions may be inferred for the barley field. It should be noted that the root mean square error values given refer to all 24 hour values. The worst fit occurs at night, when least evapotranspiration occurs. Root mean square error values for daytime only would therefore be much below the values in the tables.

A test of the accuracy of the results is shown in Table 2, which compares the estimates of hourly evapotranspiration from the model with estimates produced using an eddy correlation technique (B. A. Callander, pers. commun., 1980). Eddy correlation methods have several possible sources of inaccuracy, because of instrument errors and atmospheric stability problems; B. A. Callander (pers. commun., 1980) associated root mean square errors with his estimates which are reproduced in Table 2. The eddy correlation techniques produce large errors at night under low-wind-speed stable conditions, and so only daytime estimates are made. It may be seen that the model estimates are within the allowable errors on the eddy correlation estimates, assuming 95% confidence intervals, but that the model estimates are consistently higher

than the eddy correlation estimates. This is probably due to the very simple way in which the eddy correlation method used partitioned the estimated fluxes. The net radiation was measured, and the sensible heat flux was estimated using wind and temperature data. The soil heat flux was estimated using wind and temperature data. The soil heat flux was estimated as a fixed proportion of the net radiation, the the latent heat flux was estimated as a remainder term using Eq. (1). Consistent biasses of the latent-heat flux term are thus difficult to detect, and it should be noted that the day-to-day variations in hourly evapotranspiration rates are similar for the two estimation methods. The data for the wheat site on June 21 are modelled using a resistance formulation (Monteith, 1973) using crop resistance data from June 20, and so there are additional errors on this "eddy correlation" estimate, as reflected in Table 2.

These results show that the good agreement which can be found between measured and estimated surface temperatures leads to reasonable evapotranspiration estimates. There is also the suggestion that remote sensing of the surface soil moisture could reduce the errors of estimating the cumulative daily evapotranspiration. However, there are many assumptions inherent in this analysis, and these should be examined.

First, the area examined was evaporating and transpiring under relatively unstressed conditions, reducing the effects of stomatal resistance. A constant C_1 does reasonably well for fitting the wheat data for 3 days. However, it is necessary to use further data sets taken under stressed conditions to see how frequently the bulk diffusion coefficient C_1 needs to be re-estimated in order to give reasonable estimates of the daily cumulative evapotranspiration, and to see the assistance that surface soil-moisture data may give to reduce the errors of the estimates.

SAMPLING INTERVAL REQUIRED ON METEOROLOGICAL DATA

One of the characteristics of the remotely sensed data is that it is available repetitively for large areas. It thus provides a good way of getting estimates of hydrological variables over large areas that are very difficult or expensive to get by other methods. However, it is important that the requirements for ground data not be excessive, or the use of the remotely sensed data becomes rather superfluous. The requirement for ground meteorological data to accompany the satellite data is examined here. The meteorological data (air temperature, vapour pressure, and wind speed in the boundary layer, and optionally the components of the net radiation at the soil surface) are used to evaluate the surface heat balance equation fluxes. It is the strong dependence of these fluxes on the surface temperature which allows that measurement to be used for model calibration.

Camillo and Gurney (1984) studied the sensitivity of evaporation estimates produced by the numerical model of the atmospheric boundary layer and upper soil to random errors and constant biasses in the meteorological inputs, using the same data from West Germany described above. It was found that for the bare soil the errors in the net radiation had the most significant effect on the evaporation estimates while for the wheat field the effects of errors

in the vapor pressure and the air temperature were as important as the effect of errors in the net radiation. Bias errors were found to produce larger errors than random errors of the same magnitude for both fields.

Plots and tables of evapotranspiration errors as a function of the meteorological data random and bias errors were computed. The next stage in this sensitivity analysis is to relate these maximum allowable errors on the meteorological inputs, as determined from the maximum evaporation errors which may be tolerated for the application in mind, to the temporal and spatial sampling frequencies of the meteorological input data. This may be done using the spatial and temporal auto-correlation structure of the meteorological variables, which allows cross-correlations between variables and spacetime trade-offs to be considered (Jones et al., 1979). However, it is also of interest to examine the temporal sampling problem separately from the spatial sampling problem. This was done here by running the model with various sampling intervals on the meteorological data and then comparing the resultant errors on the evaporation.

SENSITIVITY STUDY METHODOLOGY

The baseline run used data integrated over five-minute intervals from an automatic weather station. This had been shown by Gurney and Camillo (1984) do agree well with eddy correlation estimates of evaporation. The results from all other simulations are compared to this baseline run.

Two different methods were used for acquiring meteorological data to be used in the simulations. First, the actual data were reduced to one value representing a fixed time interval. Two reduction methods were used; sampling the five-minute data at the middle of the interval, and averaging the five-minute data throughout the interval, as follows:

a) Samples: Single values to represent one, three and six hour intervals were taken from the data set. Thus, one five-minute value was taken to represent net radiation, air temperature and vapor pressure. The five-minute data from the middle of each period was used for the sample data. Where the mid-point fell at the end of a five minute sample period, the five minute period immediately preceding the mid-point was used. Anemometers are usually coupled to integrating recording instruments, so the average wind speed throughout the period was used.

b) Averages: One, three and six-hour averages were taken from the data set. This is in many ways a method more analagous to those becoming operational, where integrating recorders are used to get more representative values of all the meteorological variables, not just the wind speed. The hourly averaged data are shown in Figure 1 to illustrate the way the meteorological data vary.

Second, we tested some commonly used algorithms either to model unmeasured data or to interpolate between infrequently measured values. These models are described below.

SENSITIVITY STUDY RESULTS

Sampling and Averaging

Table 3 shows cumulative daily evaporation for the three days for the baseline, sampling, and averaging runs. It is immediately apparent from Table 3 from a comparison of the baseline and hourly average runs that, for all the three days, using hourly averaged data gives virtually identical results to the baseline. The three and six hourly averages are less good but still adequate, with the respective maximum daily variations from the baseline values being .10 mm and .15 mm respectively.

The hourly sampled data also gave adequate results, the largest error in evaporation being .14 mm. However, sampling at three and six hour intervals gave unacceptably large evaporation errors with minimum daily errors of 0.80 mm and 0.57 mm respectively.

For each of the three time intervals averaging gives more accurate evaporation estimates than does sampling. This is to be expected, as the sampling technique could easily miss fluctuations such as passing clouds which affect evaporation rates, whereas the averaging technique includes these effects to some extent.

Interpolation and Modeling

Closely related to sampling and averaging is the idea of using sparse measurements in the model. We have examined commonly used methods for using sparse measurements of air temperature, vapor pressure and wind speed, and for using net radiation models when no net radiation data are available. The data used are those reported in standard meteorological reports from secondary meteorological stations. We discuss each data type in turn. Results are shown in Table 4.

Air Temperature

Linear interpolation between the daily minimum and maximum values is commonly used to provide estimates of the air temperature at other times of the day. We have modified this algorithm to include the 9 a.m. temperature, as this value is also usually available. We therefore linearly interpolate between the daily minimum and 9 a.m., 9 a.m. and the daily maximum, and then to the next daily minimum. The evaporation estimates derived from using this 16 scheme for the air temperature are in the second column of Table 4. The third column shows the results when, instead of the true times of the extrema, the minimum and maximum are assumed to occur at 5 a.m. and 1 p.m. respectively.

A comparison of the two shows that there are no significant differences between the daily evaporation from the two schemes. If one is to use this method, the simpler case of assuming a fixed time for the daily extrema could be adopted, particularly as most synoptic reports of temperature maxima and minima do not include the time of these extrema.

The evaporation errors, which do not exceed .4 mm in any one day, should be acceptable for most applications.

Wind Speed

For an unattended weather station only the daily wind run may be available, so we have examined the use of one daily average wind speed. The results are shown in the fourth column of Table 2. Comparison to the baseline run shows good agreement for the first simulation day and progressively worse results for the next two days, for which evaporation was underestimated by .8 and 1.2 mm respectively. The reason is that for the first day the daily average, 129 cm sec^{-1}, happened to represent the wind speed for all daylight hours when evaporation is greatest (Figure 1). However, the second and third day averages were 70 cm sec^{-1} and 90 cm sec^{-1} respectively, and a comparison of these numbers to the hourly averaged data in Figure 1 shows that they grossly underestimate the wind during the periods of greatest evaporation.

These results are not surprising, as the correlation between wind speed and high evaporation is well known. The lesson applicable to data sampling is that the deviations from the mean must be small over the averaging interval. If only the daily wind run is available, it may be possible to use other meteorological data (such as the times of the passage of fronts) to reconstruct some of the variations in wind speed within the day and thereby improve evaporation estimates.

Net Radiation

It is possible to use a numerical model for the net radiation if measurements are not available. As models of this sort are commonly used, it is important to assess the effect of their use on evaporation estimates. The model used here may be summarized as follows (Eagleson, 1970):

$$R_{net} = (1-a)\ I_o\ \sin\alpha\ \exp(-.128\ n/\sin\alpha) + \sigma\varepsilon_s\ E_a\ T_a^4 - \sigma\varepsilon_s\ T_s^4 \qquad (18)$$

where a is the albedo, I_o is the solar energy flux at the top of the atmosphere (120 cal cm^{-2} hr^{-1}), α is the angle between the sun and the local tangent plane, n is a factor relating to atmospheric scattering of visible and near infrared radiation, σ is the Stefan-Boltzmann constant, ε_s is the surface emissivity, and E_a is the emissivity of the air, which may be modelled as a function of the atmospheric vapor pressure and/or air temperature. The surface dependent parameters, the albedo and emissivity, were measured with values of .18 and .96 respectively. The attenuation factor, n, was treated as a fitting parameter, the only one used in the radiation model. Figure 1 shows the hourly averaged data (solid line) and the best fit (dashed line) for n = 3, as determined by eye.

The irregularities in the data not reproduced by the model are due to cloudy conditions, which were not modelled but could be easily included as an extra factor in Eq. (18). On a daily averaged basis, June 19 was considered completely cloud covered, June 20 about 40% cloud covered, and June 21 about

15% cloud covered. The distribution over time on June 21 (the only day for which such data are available) was 25% at 11 a.m., 60% from 1 p.m. to 4 p.m., and 10% after 6 p.m. This cloud distribution is reflected in the differences between the measured and modelled net radiation in Figure 1.

The effect of these inaccuracies is tabulated in column 5 of Table 4. The deviations of the estimated evaporation from the baseline for the three days are 1 mm, -.54 mm and -.75 mm respectively.

Vapor Pressure

The 9 a.m. vapor pressure is widely available, so we have examined the errors in evaporation from using this value throughout the day. The hourly averaged values are plotted in Figure 1. The 9 a.m. values for the three days were 14.7 mb, 17.8 mb, and 22.4 mb, and column 6 of Table 4 shows the evaporation estimates. The deviations from the baseline values for the three days are .3 mm, -.4 mm, and -1.0 mm. Thus, we conclude that using the 9 a.m. measurement throughout the day when the daily variations are large (i.e. 10 mb on June 21) gives evaporation estimates with unacceptably large errors.

This sensitivity to the vapor pressure is a direct result of the important role it plays in the diffusion model, Eq. (2). Previous work (Camillo and Gurney, 1984) has shown that in a diffusion model of this type, vapor pressure errors can be as important as net radiation errors.

Vapor Pressure and Temperature

In the absence of advection, vapor pressure changes very closely with the air temperature. It is thus of interest to see the errors where the vapor pressure is calculated with the psychrometric equation, using the 9 a.m. wet bulb temperature throughout the day and the interpolated air temperature. This should give more acceptable errors than using one value for the vapor pressure throughout the day. It may be seen from Table 4 that the errors on evaporation are .5 mm, .0 mm and 0.4 mm, which should be just acceptable for many applications.

All Variables Modelled or Interpolated

It is also of interest to see how well the model performs when the net radiation is modelled and when the other meteorological data are all interpolated from sparse measurements. The air temperature was interpolated using assumed times for the maxima and minima, and the vapor pressure was calculated with the aid of the interpolated air temperature and 9 a.m. wet bulb temperature. It may be seen that the resultant errors in daily evaporation for the three days are 1.1 mm, .0 mm and .9 mm, respectively. The errors on two of the days are thus unacceptably high.

SENSITIVITY ANALYSIS DISCUSSION

We have examined the sensitivity of evaporation estimates from an energy and moisture balance model to various ways of obtaining the meteorological data

which drive the model. First, we have examined the use of averaged and sampled data, with varying time intervals represented by each data point. Hourly averages gave virtually identical results to the baseline run, in which 5 minute averages were used. Hourly sampled data gave less good but adequate results. For all intervals averaging the data gave smaller errors than did sampling so that errors from averaging over three and six hour intervals also gave acceptable results.

We also considered various other commonly used methods for providing the meteorological data. Using one average wind speed throughout the day was acceptable only when the fluctuations from this mean value were small. A linear interpolation scheme to calculate the air temperature from the daily minimum, 9 a.m., and maximum values provided acceptable results. Use of standard net radiation models could be adequate for clear sky conditions, or if they included a factor for reducing the solar radiation during cloudy conditions; this would require cloud distribution data throughout the day. We found that using the 9 a.m. vapor pressure throughout the day gave unacceptably large evaporation errors, but using the 9 a.m. wet bulb temperature and the hourly temperature interpolated from maxima, minima and 9 a.m. values gave much improved results and yielded acceptable errors. Using these interpolation and modelling algorithms together gave unacceptable results on two of the three days. However, it should be noted that these algorithms were very simplified, and somewhat more realistic algorithms, as discussed above, using ancillary data from meteorological satellites for cloud cover, or numerical weather analysis for other variables, could yield much more acceptable results. It is interesting that the results are as good as they are for such sparse data, and gives hope that the approach is reasonable for operational purposes using remotely sensed data.

ACKNOWLEDGEMENTS

Dr. R. J. Gurney is funded by NASA Goddard Space Flight Center under Grant NAG 5-9. Dr. P. J. Camillo is funded by NASA Goddard Space Flight Center under Contract NAS5-23450.

REFERENCES

1. Camillo, P. J. and R. J. Gurney, "A Sensitivity Analysis of a Numerical Model for Estimating Evapotranspiration," Water Resources Research, V. 20, 1984.

2. Camillo, P. J. and T. J. Schmugge, "Estimation of Soil Moisture Storage in the Root Zone from Surface Measurements," Soil Science, V. 135, pp. 245-264, 1983.

3. Camillo, P. J., R. J. Gurney, and T. J. Schmugge, "A Soil and Atmospheric Boundary Layer Model for Evapotranspiration and Soil Moisture Studies," Water Resources Research, V. 19, pp. 371-380, 1983.

4. Eagleson, P. S.,"Dynamic Hydrology," McGraw-Hill, New York, 1970.

5. Hillel, D.,"Fundamentals of Soil Physics," Academic Press, New York, 1980.

6. Jones, D. A., R. J. Gurney, and P. E. O'Connell, "Network Design Using Optimal Estimation Procedures, Water Resources Research," V. 15, pp. 1801 -1812, 1979.

7. Molz, F. J. and C. M. Peterson, "Water Transport from Roots to Soil," Agronomic Journal, V. 68, pp. 901-904, 1976.

8. Monteith, J. L., "Principles of Environmental Physics," American Elsevier, New York, 1973.

9. Rosema, A., J. H. B'jleveld, P. Reiniger, G. Tassone, R. J. Gurney, and K. Blyth, "Tellus, a Combined Surface Temperature, Soil Moisture and Evaporation Mapping Approach," Proceedings of the Environmental Research Institute of Michigan Symposium on Remote Sensing, Ann Arbor, Michigan, 12th, pp. 2267-2276, 1978.

10. Schmugge, T. J., T. J. Jackson, and H. L. McKim, "Survey of Methods for Soil Moisture Determination," Water Resources Research, V. 16, pp. 961-979, 1980.

11. Shuttleworth, W. J., "A One-Dimensional Theoretical Description of the Vegetation-Atmospheric Interaction," Boundary Layer Meteorology, V. 10, pp. 273-302, 1976.

12. Soer, G. J. R., "Estimation of Regional Evapotranspiration and Soil Moisture Conditions Using Remotely Sensed Crop Surface Temperature," Remote Sensing of the Environment, V. 9, pp. 27-45, 1980.

13. van der Ploeg, R. R., G. Tassone, and J. von Hoyningen-Huene, "The Joint Measuring Campaign 1979 in Ruthe (West Germany), Description and Preliminary Data, European Economic Community, Joint Research Centre, Ispra, 1980.

Table 1 - Root mean square errors between measured and estimated surface temperatures (K) for both wheat and barley fields.

	C_1					
	0.5	1.0	1.5	2.0	2.5	3.0
WHEAT						
Site D:						
June 19, 1979	1.4	1.1	1.1	1.1	1.2	1.2
June 20, 1979	2.2	1.8	2.2	2.3	2.6	2.6
June 21, 1979	2.2	1.5	2.1	2.5	2.6	2.5
Site G:						
June 19, 1979	2.0	1.4	1.2	1.1	1.1	1.1
June 20, 1979	3.9	2.3	1.7	1.6	1.5	1.4
June 21, 1979	4.2	2.2	1.6	1.2	1.0	0.9
BARLEY						
Site K:						
June 19, 1979	1.6	1.1	1.1	1.1	1.1	1.2
June 20, 1979	2.6	1.4	1.4	1.6	1.6	1.7
June 21, 1979	3.3	3.6	3.9	4.1	4.2	4.3
Site I:						
June 19, 1979	2.3	1.6	1.4	1.3	1.2	1.3
June 20, 1979	3.6	2.0	1.6	1.4	1.3	1.3
June 21, 1979	3.5	1.8	1.2	1.1	1.0	1.1

Table 2 - Comparison of eddy correlation and energy balance model estimates of hourly evaporation rates (mm $hr.^{-1}$).

	Eddy Correlation	Root Mean Square Error	Energy Balance
Wheat:			
June 19, 1979	0.239	0.061	0.233
June 20, 1979	0.280	0.104	0.438
June 21, 1979	0.411	0.146	0.531
Barley:			
June 19, 1979	0.149	0.086	0.267
June 20, 1979	0.325	0.110	0.481
June 21, 1979	0.354	0.112	0.470

Table 3 - Cumulative daily evaporation (mm) for three days, for the baseline run and runs using various averaging and sampling intervals.

Date	Baseline	Hourly Average	3-Hourly Average	6-Hourly Average	Hourly Sample	3-Hourly Sample	6-Hourly Sample
June 19	3.24	3.26	3.25	3.17	3.19	3.47	3.78
June 20	5.31	5.32	5.24	5.16	5.21	6.11	5.88
June 21	6.94	6.93	6.84	6.79	7.08	6.17	7.46
3 Day Total	15.49	15.51	15.33	15.12	15.48	15.75	17.12

Table 4 - Cumulative daily evaporation (mm) for three days, for the baseline run and for runs using various methods to use sparse data (air temperature, vapor pressure, wind speed) or model non-existent data (net radiation).

A: Baseline run.

B: Air Temperature linearly interpolated between daily minimum, 9 a.m. temperature and daily maximum, with true times of minima and maxima.

C: Air temperature linearly interpolated between daily minimum, 9 a.m. temperature and daily maximum, with times of minima and maxima assumed at 5 a.m. and 1 p.m. respectively.

D: Daily wind run.

E: Net radiation model.

F: 9 a.m. vapor pressure used throughout day.

G: 9 a.m. vapor pressure interpolated using interpolated air temperature.

H: All variables interpolated or modelled.

Date	A	B	C	D	E	F	G	H
June 19	3.24	3.49	3.55	3.29	4.22	3.58	2.76	4.32
June 20	5.31	5.47	5.43	4.55	4.77	4.96	5.34	5.34
June 21	6.94	6.78	7.18	5.74	6.19	5.95	7.32	7.87
3 Day Total	15.49	15.74	16.16	13.58	15.18	14.49	14.41	17.53

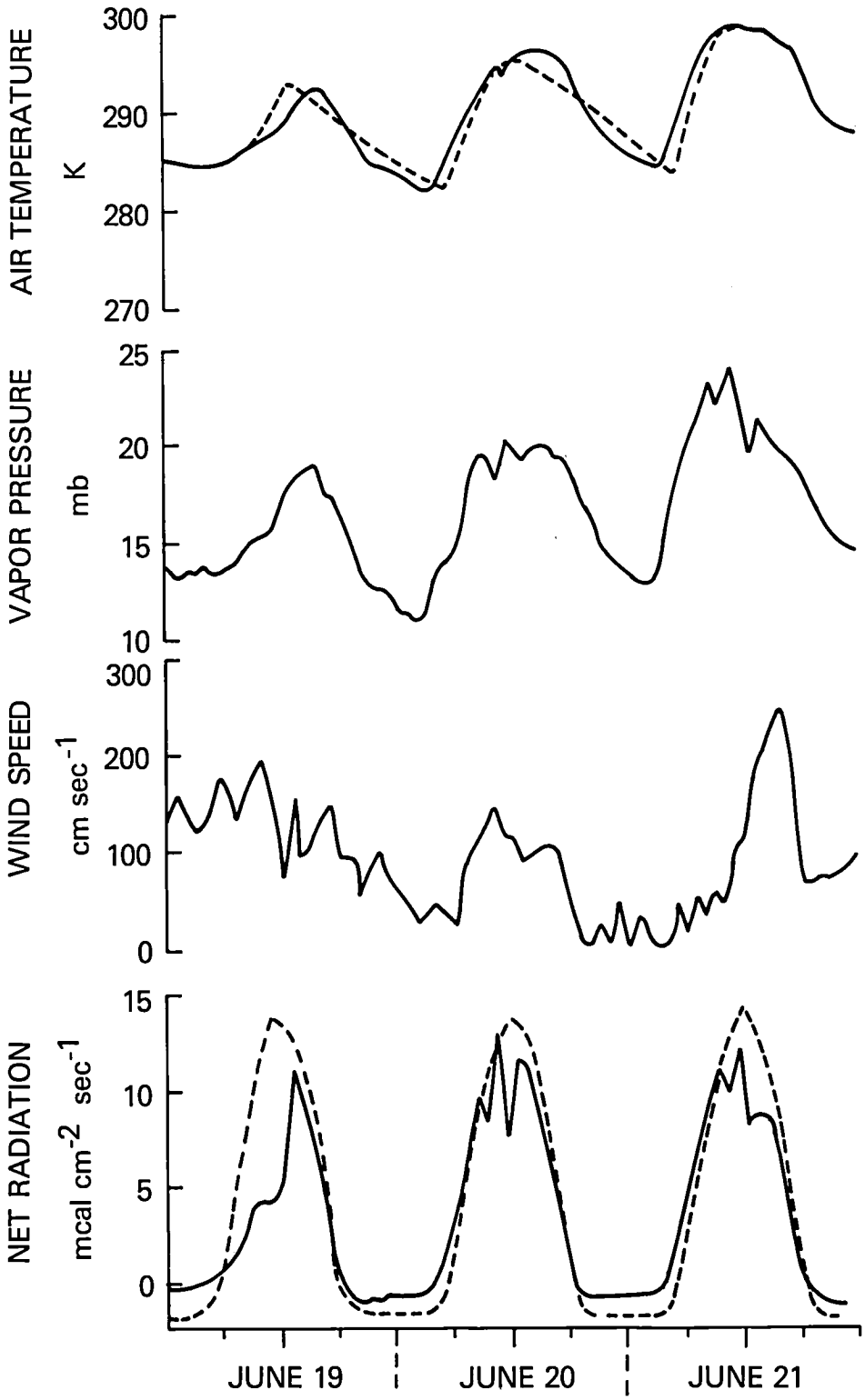

Figure 1. The meteorological input data input to the baseline run, showing air temperature, wind speed, net radiation and vapor pressure respectively. The modelled radiation data and interpolated air temperature also shown as dashed lines.